ENEA - RT/TIB/84/36

E. CUPINI, A. VENTURA

COMPARISON OF UNIVERSAL POTENTIALS FOR ATOMIC COLLISIONS IN SOLIDS

COMITATO NAZIONALE PER LA RICERCA E PER LO SVILUPPO DELL'ENERGIA NUCLEARE E DELLE ENERGIE ALTERNATIVE

ENEA-RT/TIB/84/36

E. Cupini, A. Ventura (ENEA-Dipartimento Tecnologie Intersettoriali di Base, Bologna)

COMPARISON OF UNIVERSAL POTENTIALS FOR ATOMIC COLLISIONS IN SOLIDS

Riassunto — Le collisioni elastiche nei solidi di ioni di energia cinetica superiore a qualche decina di eV possono essere descritte con ragionevole accuratezza dell'approssimazione a collisioni binarie, in cui si usano frequentemente potenziali coulumbiani schermati. Lo scopo del presente lavoro è confrontare con dati sperimentali calcoli basati sul potenziale di Molière e sul più realistico potenziale di Biersack-Ziegler per collisioni atomiche in solidi di numero atomico fra $Z = 6$ (grafite) e $Z = 79$ (oro).
Un accettabile accordo con i dati sperimentali si può ottenere, in generale, con entrambi i potenziali, modificando opportunamente la lunghezza di schermo nel caso di Molière, mentre nessun aggiustamento di parametri è necessario per Biersack-Ziegler.

ENEA-RT/TIB/84/36

E. Cupini, A. Ventura (ENEA-Dipartimento Tecnologie Intersettoriali di Base, Bologna)

COMPARISON OF UNIVERSAL POTENTIALS FOR ATOMIC COLLISIONS IN SOLIDS

Summary — *Elastic collisions in solids of ions having kinetic energy greater than about ten eV are fairly well described by the binary collision approximation, where screened Coulomb potentials are often used.*
The aim of the present work is to compare calculations based on the Molière potential and on the more realistic Biersack-Ziegler potential for atomic collisions in solids having an atomic number between $Z = 6$ and $Z = 79$ with experimental data. A reasonable agreement with data can be obtained, in general, by means of both potentials provided that the screening length is suitably modified in the Molière case, while no parameter adjustment is needed in the Biersack-Ziegler potential.

COMITATO NAZIONALE PER LA RICERCA E PER LO SVILUPPO
DELL'ENERGIA NUCLEARE E DELLE ENERGIE ALTERNATIVE

E. CUPINI, A. VENTURA

COMPARISON OF UNIVERSAL POTENTIALS FOR ATOMIC COLLISIONS IN SOLIDS

RT/TIB/84/36

Testo pervenuto in dicembre 1984

1. INTRODUCTION

Experimental and theoretical studies of the interactions of ions in broad ranges of mass and charge with crystals, polycrystals, amorphous materials is of the utmost importance in many areas of applied physics. Ion bombardment may be responsible for a variety of phenomena in irradiated targets, such as sputtering, alteration of physical properties or chemical composition. Reflection and trapping of light ions such as hydrogen, deuterium and helium, in particular, are to be carefully studied for a proper description of plasma-wall interactions in present and future fusion devices.

When the incident ion energy is high enough to make the probability of collective excitations in the target negligible, propagation of ions in matter may be thought of as a series of two-body collisions with atoms forming a rather rigid crystalline or amorphous structure. The target atoms can be displaced from their equilibrium positions, forming a cascade of interstitials and their accompanying vacancies. Numerical simulation of such displacement cascades can be simply performed within the framework of the above mentioned binary-collision approximation. Here, repulsive interactions are described by the methods of classical mechanics and use is made of simple interatomic potentials, for instance screened Coulomb potentials, whose parameters can be estimated from theory, but are usually adjusted on experimental data. This is the case of the widely-used Molière potential |1|. A more realistic treatment of atomic interactions on the basis of the Hartree-Fock-Slater approximation,for instance, cannot be directly inserted into computer codes which simulate displacement cascades, because of the very long computing time.
Thus, it is interesting to see whether parametrization of a large number of self-consistent calculations could lead to a simple universal potential to be used for any projectile-target combination without further parameter adjustment, and compare numerical simulations based on such a potential with experimental data. This is the case of the Biersack-Ziegler potential |2|, used in the present work.

2. UNIVERSAL POTENTIALS IN ATOMIC COLLISIONS

The Molière interatomic potential |1| has been used for a long time in computer simulations of atomic displacement cascades, owing to its simple expression, well suited to time-comsuming numerical applications, which reads:

$$V(r) = (Z_1 Z_2 e^2/r)\varphi(r/a_{12}) \qquad (1)$$

where Z_1 and Z_2 are the atomic numbers of the interacting species, r the interatomic distance and $\varphi(x)$ the following screening function:

$$\varphi(x) = 0.35\ \exp(-0.3x)+0.55\ \exp(-1.2x)+0.10\ \exp(-6.0x) \qquad (2)$$

As is known, formula (2) is a good approximation of the Thomas-Fermi function for small $x(\lesssim 5)$ and the screening length, a_{12}, can be estimated in the Thomas-Fermi approximation. A well-known expression derived by Firsov |3| reads:

$$a_{12} = \left(\frac{9\pi^2}{128}\right)^{1/3} \frac{a_B}{\left(Z_1^{1/2} + Z_2^{1/2}\right)^{2/3}} \qquad (3)$$

where $a_B = \hbar^2/(m_e e^2)$ is the Bohr radius.

It is known, however, that two-atom potentials of the Thomas-Fermi type give a good description of repulsive interactions only for high energy projectiles, when short-range effects are dominant, but are not suited to the simulation of low-energy ion scattering, due to the fact that they fall off too slowly at large interatomic distance.
It is, therefore, common practice to use Molière potentials with screening lengths somewhat reduced with respect to the theoretical value (3) in computer simulations of low-energy ion scattering.

On the other hand, the interaction energy of two colliding atoms can be calculated with more realistic models: for instance, the Hartree-Fock-Slater approximation has been used in ref. |4| to study more than five hundred projectile-target combinations. The individually calculated interaction potentials cannot be fitted by a Molière function.

For medium heavy ions and targets the Authors of ref. |4| proposed the so-called "krypton-carbon" screening function:

$$\varphi_{Kr-C}(x) = 0.1909\ e^{-0.28x} + 0.4737\ e^{-0.64x} + 0.3354\ e^{-1.9x}, \qquad (4)$$

with a screening length of the Firsov type (3).

This "medium" case, however, does not fit the interaction energies of the lightest, or heaviest species considered in ref.|4| very well , that is why, in ref. |2|, Biersack and Ziegler consider the special

case of homoatomic interactions ($Z_1 = Z_2$) first and allow the various contributions to the total interaction energy to have different Z dependence: the Coulomb interaction energy between the two atoms, V_c, and the kinetic energy increase of the electrons, V_k, due to the increased electron density in the overlap region of the two atoms, turn out to be proportional to $Z^{7/3}$:

$$V_1 = V_c + V_k = \frac{Z^{7/3}}{R} \cdot \varphi_1(x) \tag{5}$$

Here, $R = Z^{1/3} r$, with r interatomic distance, and φ_1 is obtained from a fit to the Hartree-Fock-Slater V_1 terms in the form:

$$\varphi_1(x) = 0.09\exp(-0.19x) + 0.61\exp(-0.57x) + 0.30\exp(-2x) \tag{6}$$

The argument of φ_1 is $X = r/a$, with a screening length of the Firsov type (3):

$$a = \left(\frac{9\pi^2}{128}\right)^{1/3} \cdot \frac{a_B}{2^{2/3} Z^{1/3}} \tag{7}$$

At large atomic separations, up to about 50% of the total interaction energy can be contributed by exchange and correlation energies, due to the local repulsion of equal spins and charges of electrons.

Fitting the Hartree-Fock-Slater exchange-plus-correlation energies from ref.[4], Biersack and Ziegler obtain the following expression:

$$V_2 = V_{exc.} + V_{corr.} = -\frac{Z^{5/3} e^2}{R} \varphi_2(R) \tag{8}$$

where $R = Z^{1/3} r \simeq 0.295\ r/a$, and $\varphi_2(R)$ is the following function:

$$\varphi_2(R) = 0.07 \exp\left(-\frac{1}{49 R^2} - \frac{R}{4} - \frac{R^2}{49}\right) \tag{9}$$

Thus, the total interaction energy of two colliding atoms of the same type can be written in the form:

$$V \equiv V_1 + V_2 = \frac{Z^2 e^2}{r}\left[\varphi_1(x) - Z^{-2/3}\varphi_2(0.295x)\right] \qquad (10)$$

Formula (10) is the expression of the Biersack-Ziegler potential for the homoatomic case ($Z = Z_1 = Z_2$). A comparison of Molière and Biersack-Ziegler functions is shown in Fig.1.

In the the heteroatomic case ($Z_1 \neq Z_2$) there are no simple extensions of formula (10), but the best potential has been obtained through the geometric mean of the homoatomic potentials, V_{11} and V_{22}, corresponding to Z_1 and Z_2, respectively.

$$V_{12}(r) = \sqrt{V_{11}(r)\cdot V_{22}(r)} = \frac{Z_1 Z_2 e^2}{r}\sqrt{\left(\varphi_1^{(1)} - Z_1^{-2/3}\varphi_2^{(1)}\right)\cdot\left(\varphi_1^{(2)} - Z_2^{-2/3}\varphi_2^{(2)}\right)} \qquad (11)$$

where the symbols are self-explanatory.

3. THE "MARLOWE" CODE

Ion reflection and trapping, displacement cascades and sputtering under ion bombardment can be simulated by means of widely used computer codes, such as TRIM [5], fast and efficient, but limited to amorphous (uniform density) targets, or MARLOWE [6], more time-consuming, but able to deal with crystals and polycrystals, too.

Version 11 of MARLOWE has been modified for use in the present work. The underlying physical model, thoroughly discussed in ref. [6], is the binary-collision approximation, namely the description of the trajectory of a particle moving in a solid as a series of two-body collisions, an assumption valid at high velocity, when the traveling particle sees the individual atoms of the lattice and no longer valid below a critical velocity, roughly that of the longitudinal (sound) waves in the solid, when the particle begins to give rise to strong many-body effects. The corresponding critical energy can be of the order of 10 to 30 eV for a number of metals, quoted in ref. [6].

During the motion of the primary particle, collisions could transfer enough energy to target atoms to displace them permanently from their equilibrium positions in the lattice: if the transferred energy is greater than a preassigned value, E_d, they are added to the cascade.

When the energy of an atom falls below a predetermined lower limit E_c, or when it escapes from the target, it is dropped from the cascade.

When no more particles remain to be followed, a number of analyses of the numerical results are carried out.

The number of histories, or primary particles to be followed, depends on the quantity of interest: for example, 1000 histories can supply rich enough statistics for the evaluation of a particle reflection coefficient, but at least 10,000 histories are necessary to investigate the angular and energy distributions of reflected particles.

Coming now to further details about the model of binary collisions, it is to be pointed out that particles are assumed to move along straight-line segments, corresponding to the asymptotes of their paths in the laboratory system. Elastic scattering by repulsive potentials is described within the framework of classical mechanics. Inelastic energy losses, due to the excitation of electrons of the medium, can be added to the elastic ones in various approximations: they can be assumed non-local and described in terms of continuous energy losses per unit path length, according to Firsov |7|, or Lindhard and Scharff |8|. Local energy losses can be treated as functions of impact parameter as in refs. |6| and |9| by proper modifications of models |7| and |8|, respectively.

As for the target structure, MARLOWE simulates a polycrystal by random rotation of a portion of perfect crystal around a lattice site at the beginning of each history and an amorphous material by random rotation of the crystal before each collision: the target density is thus conserved, but directional correlations are weakened in the former case, almost cancelled in the latter.

The main change we have made in the MARLOWE version at our disposal has, of course, been the introduction of the Biersack-Ziegler potential. Some caution is needed in numerical applications, since the Biersack-Ziegler screening function is not positive definite and is to be put equal to zero at large interatomic distances, where formula |11| could yield a negative value, and make the approximation meaningless.

4. NUMERICAL RESULTS: GOLD ON GOLD

Our first comparison of computer simulations based on the Moliere and the Biersack-Ziegler potentials involves homoatomic interactions in the damage profiles for 250-keV self-ion irradiation of gold, described in ref. |10|. In this experiment thin gold films of (001) orientation were irradiated at room temperature ($\sim$ 293°K) with 250-keV Au^+ ions to a dose of 3×10^{16} ions/m^2. The specimens were mounted on a rotating target holder and, in order to sample a range of incident beam directions and minimize possible channeling, they were rotated about an axis 15° $\pm$ 5°

from the ⟨001⟩ axial and 22° ± 5° from the planar channel. The depth distribution of defect clusters produced by irradiation was determined by stereo electron microscopy. In the same paper a computer simulation of damage profiles in gold was performed using the MARLOWE code: atomic collisions were described by the Molière potential and inelastic energy losses by the local-modified Firsov formalism of ref. |6|.

The Authors of ref. |10| were, of course, aware that a direct comparison of the experimental distribution of visible defect clusters with a simulated distribution of point defects was to be considered with caution. For instance, only clusters above a certain size, of the order of 20 to 50 point defects, are visible. Moreover, point defects are mobile at room temperature and their distribution in depth after migration and rearrangement does not necessarily reflect the distribution of the defects directly produced by irradiation. There is, however, for irradiated gold, experimental evidence that defect clusters greater than 20 Å in diameter are directly produced in energetic displacement cascades and that processes involving the long-range migration of defects can be excluded |11|. The comparison |10| of experimental and simulated damage profiles is therefore of some use for testing the simulated target structure and the chosen interatomic potential. The main conclusions of ref. |10| are that the best agreement between simulation and experiment is obtained in polycrystalline approximation, including thermal lattice vibrations ruled by a Debye temperature ϑ_D = 162.4 °K and describing gold-gold collisions by means of a Molière potential with a screening length, a_s = 0.053 Å, of the order 77% a_F where a_F = 0.069 Å is the theoretical Firsov value for gold-gold interactions, derived from formula (3).

In order to check our computational procedure we have repeated the simulation of ref. |10| for a gold polycrystal, keeping the same input values for MARLOWE: the 250-keV gold ions enter the crystal surface at ϑ=15° with respect to the normal, thermal vibrations of the gold lattice at T = 293 °K being taken into account; atomic collisions are described by a Molière potential with screening length a_s = 77% a_F; the largest impact parameter is p_m = 0.51 a, where a=4.079 Å is the gold lattice constant; the minimum energy of displacement is E_d = 43 eV and the cut-off energy below which an atom is dropped from the cascade is E_c = 86 eV.

The relative number of vacancies per unit depth, obtained from 200 histories, is plotted in Fig.2 as a function of depth (in units of the lattice constant) and compared with the experimental depth distribution of vacancy clusters from ref. |10|. The two histograms are normalized at their maximum.

The same calculations have been repeated with the Biersack-Ziegler potential, whose screening length is equal to the theoretical Firsov value for gold, $a_F = 0.069$ Å. No other changes have been made in the input parameters. The damage profile calculated by means of the Biersack-Ziegler potential is also compared with the experimental one in Fig.2. Both the calculated profiles show a rather broad maximum at about 30a while the experimental one is slightly shifted towards 40a; Molière seems to work better than Biersack-Ziegler up to 120 a, while the opposite trend appears at greater depths. It is, however, to be pointed out that our statistics are not rich enough to describe the distribution tails correctly. In conclusion, both potentials yield a reasonable damage profile, but the Molière screening length has been adjusted "ad hoc", while no modification is needed in the Biersack-Ziegler case.

5. HELIUM ON GOLD

A test of the Biersack-Ziegler formula for heteroatomic interactions, in this case light projectiles on heavy target, is supplied by the simulation of backscattering of 16-keV helium ions from gold, to be compared with the experimental data and the TRIM simulation of ref. |12|. In that work, a clean, polycrystalline gold target was bombarded with hydrogen and helium ions in the 5-16 keV energy range at normal incidence; the angular and energy distributions of backscattered particles were determined. The measurements were performed at various exit angles (with respect to the surface normal) between 25° and 90°. Since a non negligible fraction of emerging particles was expected to be neutral, they were ionized in a gas stripping cell prior to energy analysis in an electrostatic spectrometer and detection in a channeltron multiplier. In the case of helium the efficiency of the stripping cell was much lower than for hydrogen over a large energy range and completely unknown below 0.8 keV. Therefore, the helium spectra have larger statistical errors than the hydrogen spectra and are not measured at all below 0.8 keV. By determining the number and the energy, E, of helium ions emitted in a ring-shaped solid-angle interval of width $\Delta\beta$ around a given exit angle, β, the Authors of ref. |12| succedeed in estimating the intensity $F(E,\beta)$, defined as the number of particles reflected per incident particle, per energy interval and per steradiant. Integrating $F(E,\beta)$ over the solid angle corresponding to the whole half-space yields the energy distribution, F(E), of the reflected particles; integrating $F(E,\beta)$ over the energy, E, from 0 to the primary energy, E_0, and multiplying by the solid-angle interval $\Delta\Omega = 4\pi \sin\left(\frac{\Delta\beta}{2}\right) \sin\beta$ yields the angular distribution, $G(\beta)$, of the reflected particles as a function

of the exit angle β . Finally, integrating $G(\beta)$ over β from 0° to 90° yields the particle reflection coefficient, R_N.
In all the cases considered, in particular for primary 16-KeV helium, the experimental angular distribution is proportional to a cosine distribution:

$$g(\beta) = 2 \sin\beta \cos\beta, \quad (0 \leq \beta \leq 90°) \tag{12}$$

or, in terms of $t \equiv \cos\beta$:

$$f(t) = \frac{g(\beta)}{\left|\frac{dt}{d\beta}\right|} = 2t \qquad (0 \leq t \leq 1) \tag{13}$$

In the case of incident 16-keV helium the energy distribution of reflected particles, F(E), is not measured at low energy, as already mentioned, shows a broad maximum around 5.5 keV and decreases slowly up to about about 15 keV. The mean energy , $\langle E \rangle$, is 6.6 keV.

Our numerical simulations have been carried out in polycrystalline approximation, but we have also taken the MARLOWE input parameters used in ref. |13| into account to compare amorphous approximations of MARLOWE and TRIM with the experimental data of ref. |12|.

The screening length of the Molière potential for Au-He interactions has been kept equal to the Firsov value, a_F(Au-He)=0.099 Å . Inelastic energy losses are described by the non-local Lindhard-Scharff formula |8|. The maximum impact parameter in two-body collisions is p_m = 0.62 a, where a is the gold lattice constant. The displacement energy for gold atoms is assumed to be E_d = 30 eV, the cut-off energy E_c = 5 eV. These values of p_m, E_d, E_c are the same as those adopted in ref. |13|.
An analogous simulation based on the heteroatomic Biersack-Ziegler formula (11) uses the Firsov screening lengths for Au-Au and He-He interactions, namely a_F(Au-Au) = 0.069 Å and a_F(He-He) = 0.23 Å , but the same approximations and input parameters as in the previous case.

Angular and energy distributions of reflected particles, obtained from 10^4 histories, are compared to the experimental results of ref. |12| in Figs.3 and 4, respectively. The angular distributions fit the cosine law (13) quite well in both cases, while both energy distributions are somewhat flatter than the experimental curve, with a rather broad maximum shifted towards higher energy.

Assuming a smaller screening length in the Molière case could shift the maximum in the right direction, as shown in ref. |13|, but the shape of the histogram would not be improved. Therefore, neither potential reproduces the experimental energy distribution, at least in polycrystalline approximation. The particle reflection coefficient calculated by means of Molière is $R_N = 0.225$, in agreement with the Biersack-Ziegler value, $R_N = 0.250$. They are smaller than the TRIM result, $R_N = 0.283$, obtained in ref. |12|, but not small enough to reproduce the experimental value, $R_N = 0.111 \pm 0.06$, from the same reference.

6. DEUTERIUM ON GRAPHITE

After considering heavy ion - heavy target and light ion - heavy target combinations in sections 4 and 5, respectively, we turn now to a light ion - light target combination, namely deuterium in the 0.4 - 10 keV energy range impinging on polycrystalline graphite at various angles of incidence |14|.
Since the implanted deuterium does not diffuse in graphite at room temperature ($\sim$293°K) it is possible to determine the particle reflection coefficient, R_N, from the trapping coefficient, $T_N = 1-R_N$, measured as the ratio between the areal density of trapped deuterium and the known incident fluence below the saturation threshold. The amount of trapped deuterium has been measured in ref. |14| bombarding the target with a beam of 790-keV He ions and counting the protons from the nuclear reaction $D+{}^3He \rightarrow {}^4He+p$. T_N and R_N have been obtained in ref. |14| as functions of the angle ϑ of incidence of the deuterium beam with respect to the surface normal. ϑ ranges from 0° to 85°. In the same paper a TRIM simulation yields R_N values in satisfactory agreement with the experimental data. The interatomic potential used in that calculation is the "krypton-carbon" potential given in formula (4).

We have reproduced the experimental R_N's from ϑ=0° to ϑ=85° at the primary energies $E_o = 0.4$ keV and $E_o = 3$ keV using a Molière potential with a deuterium-carbon screening length $a_S(D-C) = 0.174$ Å, about 85% of the Firsov value $a_F(D-C) = 0.205$ Å. The maximum impact parameter is $p_m = 0.82a$, where $a = 2.46$ Å is the first lattice constant of graphite, the second being $c = 6.71$ Å. Inelastic energy losses have been calculated by means of the Lindhard-Scharff formula |8|. The amorphous approximation has been preferred to the polycrystal, because the latter approximation yields R_N's at intermediate incidence angles which are too small.

An analogous simulation with the Biersack-Ziegler potential uses the Firsov screening lengths $a_F(C-C) = 0.162$ Å and $a_F(D-D) = 0.295$ Å.

The other input parameters and approximations are the same as in the case of Molière. The reflection coefficients calculated on the basis of 2000 histories are compared with the experimental ones in Fig. 5. The agreement turns out to be quite satisfactory and can be considered an "a posteriori" validation of the Biersack-Ziegler formula for D-D interaction, not computed in refs. |2|-|4|.

7. ARGON ON MAGNESIUM

For the sake of completeness we quote here a comparison of the Molière and Biersack-Ziegler potentials performed in ref. |15| in order to fit experimental energy distributions of Ar^+ ions impinging on magnesium with initial energy E_o = 4 keV and multiply scattered through 30° from a (0001) surface along the $\langle 2\,\bar{1}\,\bar{1}\rangle$ and $\langle 0\,\bar{1}\,1\rangle$ directions.

The Authors of ref. |15| point out that self-consistent calculations of the Ar-Mg interaction are well reproduced over a large interval of interatomic separations by the Biersack-Ziegler potential and by the Molière potential with a screening length a_S = 85% a_T(Ar-Mg), where a_T denotes a theoretical Thomas-Fermi value. Introducing this modified Molière potential in the non-vibrating chain model used for the simulation of ion scattering in a given surface row, they find that the position of the main peak of the energy spectrum for ions scattered in the $\langle 0\,\bar{1}\,1\rangle$ direction is well reproduced, while the corresponding peak of the energy spectrum for ions scattered in the $\langle 2\,\bar{1}\,\bar{1}\rangle$ direction is placed at higher energy than the experimental peak.
In this case an even smaller screeming length, a_S = 70% a_T, would give agreement between simulations and experiment, but it is clearly inappropriate for the $\langle 0\,\bar{1}\,1\rangle$ row.

The main conclusion of ref. |15| is that the Biersack-Ziegler potential should be employed in ion-scattering simulations in preference to the modified Molière potential.

8. CONCLUSIONS

The examples of simulations of atomic interactions in solids described in the present work, though not exhaustive, make us confident that the Biersack-Ziegler potential can successfully replace the less realistic Molière potential in a large number of applications at the cost of longer computing time for heteroatomic interactions, but with the unquestionable advantage of being free of adjustable parameters. Further applications in the fields of radiation damage, ion reflection and

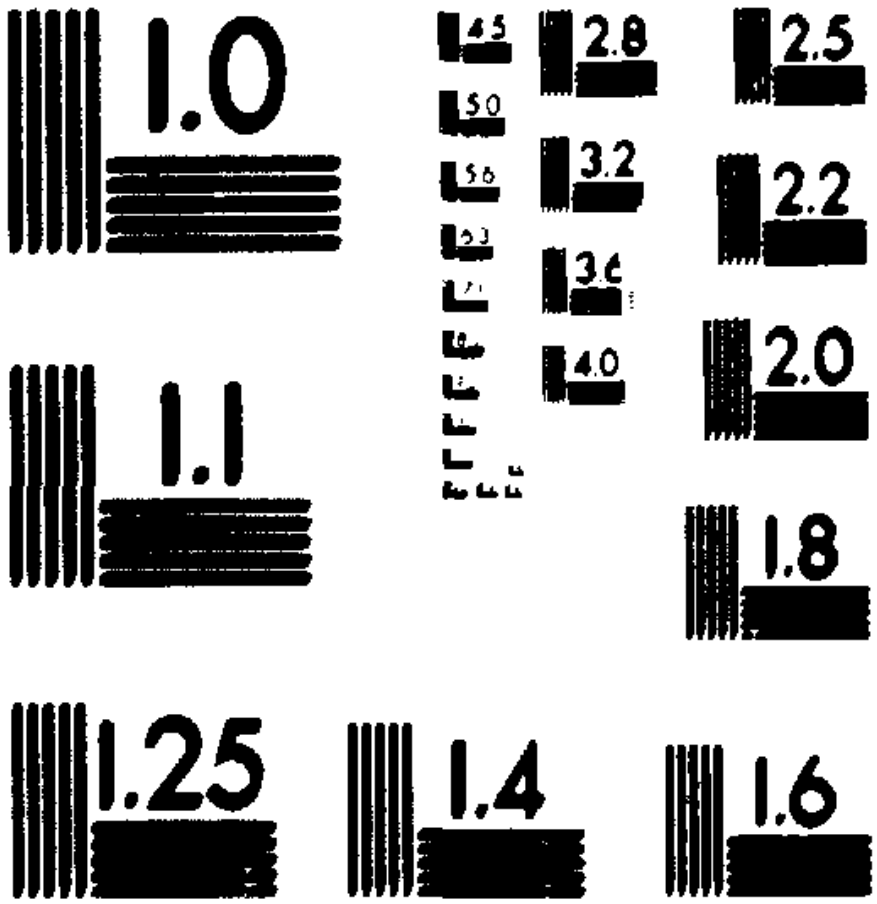

sputtering, as well as deeper theoretical studies of inelastic energy losses, which in their local form depend on the distance of closest approach between atoms, are planned for the near future.

REFERENCES

|1| G. Molière, Z.Naturforsch A, 2, 133 (1947)

|2| J.P. Biersack and J.F.Ziegler, Nucl.Instrum. Methods 194, 93 (1982)

|3| O.B. Firsov, Sov. Phys. JEPT, 6 , 534 (1958)

|4| W.D. Wilson, L.G. Haggmark, J.P. Biersack, Phys. Rev. B, 15 , 2458 (1977)

|5| J.P. Biersack and L.G. Haggmark, Nucl. Instrum. Methods, 174 257 (1980)

|6| M.T. Robinson and I.M. Torrens, Phys. Rev. B, 9 , 5008 (1974)

|7| O.B. Firsov, Sov. Phys. JETP, 9 , 1076 (1959)

|8| J. Lindhard and M. Scharff, Phys. Rev., 124 , 128 (1961)

|9| O.S. Oen and M.T. Robinson, Nucl. Instrum. Methods, 132 , 647 (1976)

|10| R. Benedek and K.L. Merkle, Radiat. Eff., 60 , 85 (1982)

|11| K.L. Merkle, Phys. Status Solidi, 18 , 173 (1966)

|12| H. Verbeek, W. Eckstein, R.S. Bhattacharya, J. Appl. Phys., 51,1783 (1980)

|13| W.Eckstein, H. Verbeek, J.P. Biersack, J. Appl. Phys., 51, 1194 (1980)

|14| C.K. Chen, B.M.U. Scherzer, W. Eckstein, Appl. Phys. A, 33, 265 (1984)

|15| S.A. Cruz, E.V. Alonso, R.P. Walker, D.J. Martin, D.G. Armour,Nucl. Instrum. Methods, 194 , 659 (1982).

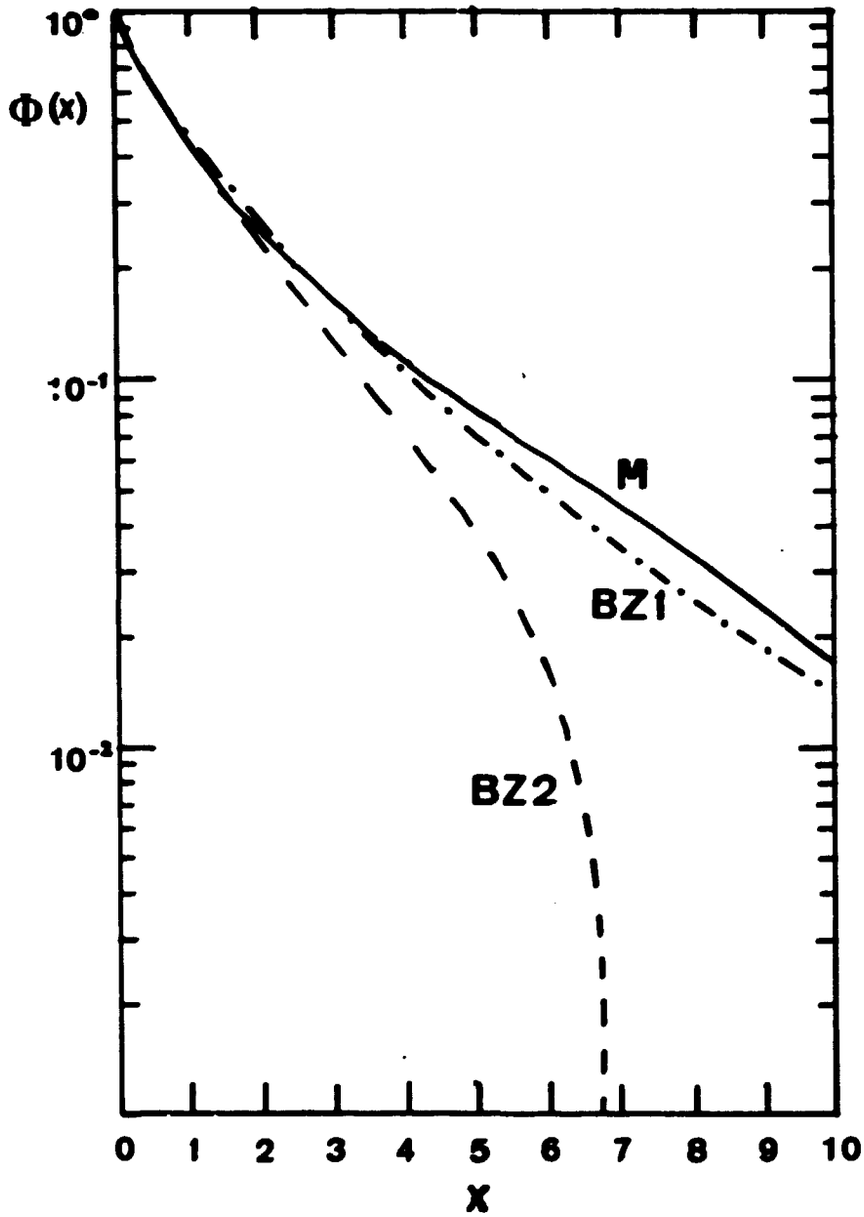

Fig.1: Screening functions versus interatomic distance x , in units of the Firsov length (formula (3)): M : Molière; BZ(Au-Au)(BZ1) : Biersack-Ziegler, for gold-gold interactions; BZ(D-C): Biersack-Ziegler, for deuterium-carbon interactions(BZ2).

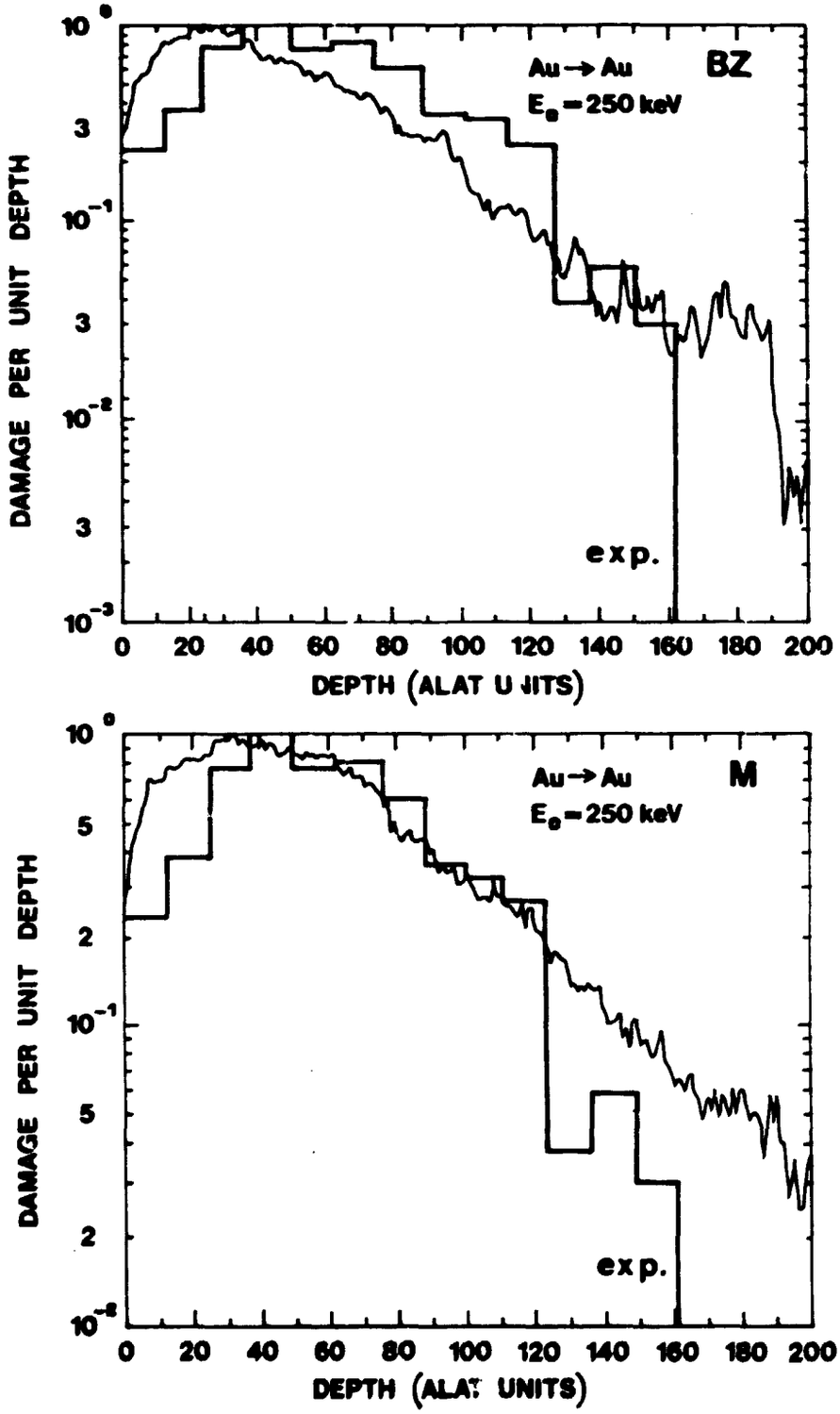

Fig.2: Distribution of vacancies per unit depth versus depth (in units of the lattice constant) for the self-irradiation of gold discussed in Section 4. BZ : damage profile calculated by means of the Biersack-Ziegler potential. M: the same profile calculated by means of the Molière potential, with modified screening length. EXP: experimental distribution of defect clusters from ref. [10]. Experimental and calculated profiles are normalized at their maximum.

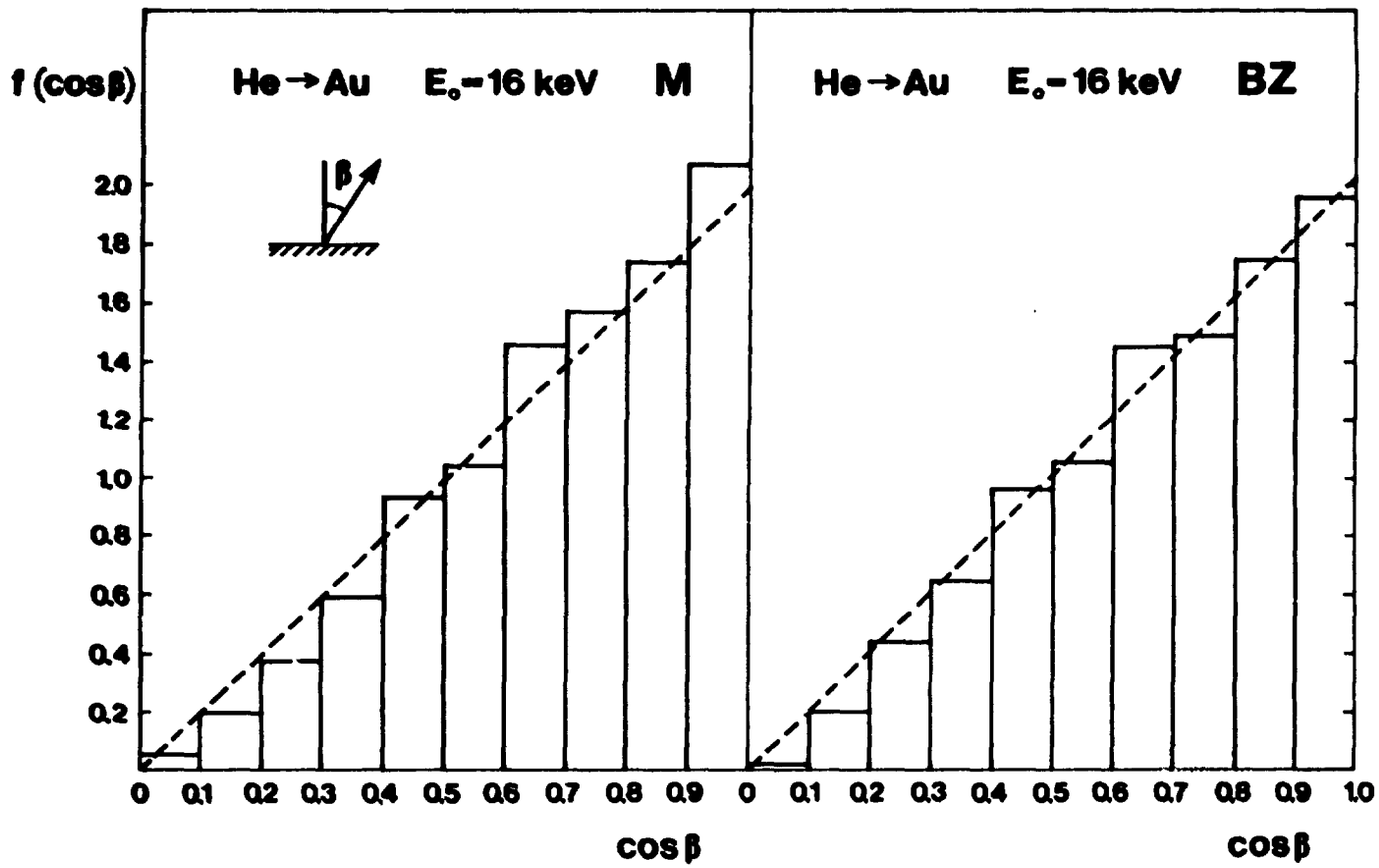

Fig.3: Angular distributions of helium backscattered from gold, discussed in Section 5. The independent variable is the cosine of the exit angle β.
The dashed lines are theoretical cosine distributions, consistent with the experimental results of ref.[12]. As in the previous figure, M means Molière, BZ Biersack-Ziegler.

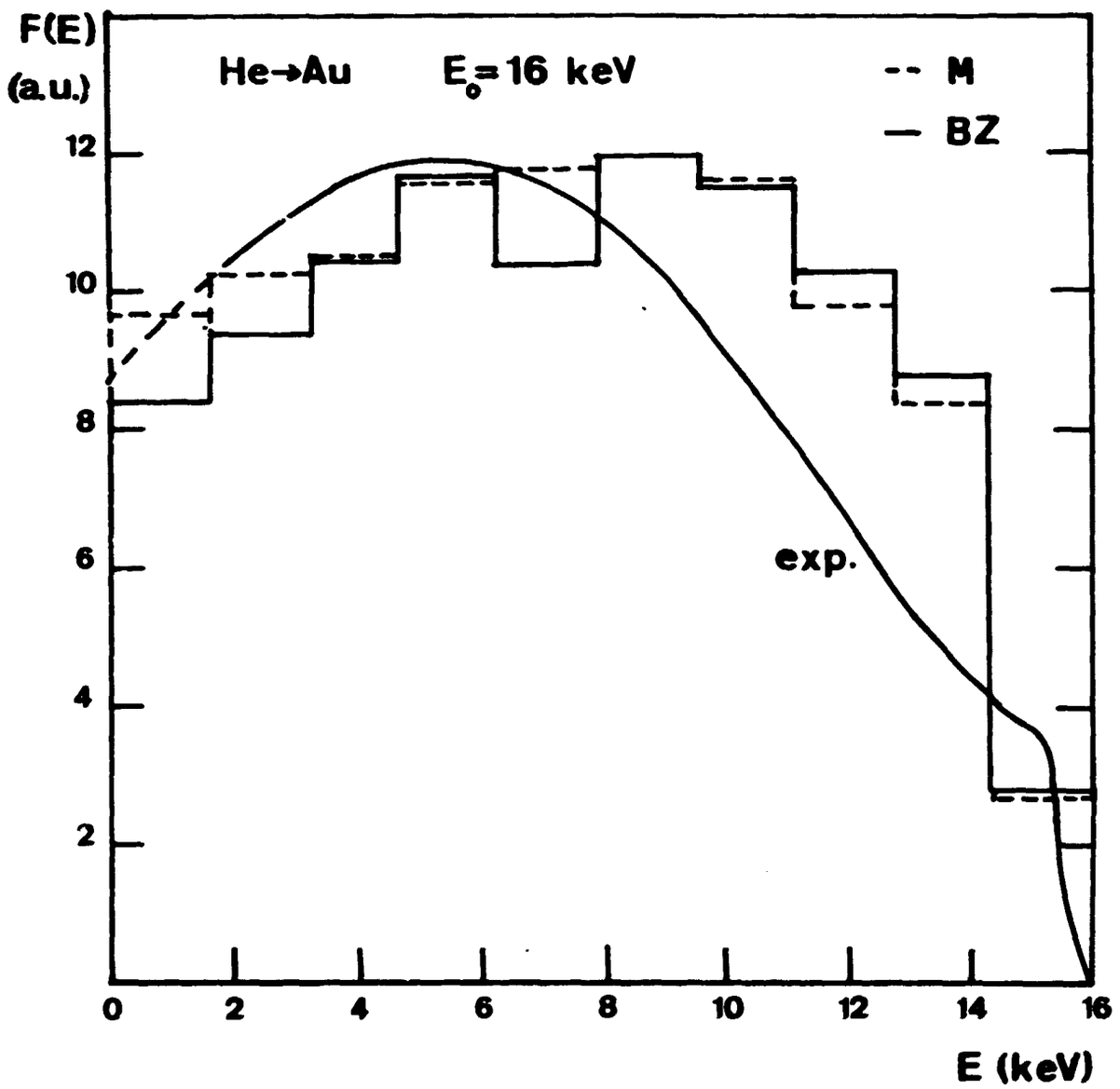

Fig.4: Energy distributions of helium backscattered from gold, discussed in Section 5. Solid curve, experimental result, from ref. |12|: dashed histogram: Molière simulation: solid histogram: Biersack-Ziegler simulation. Curve and histograms are normalized at their maximum.

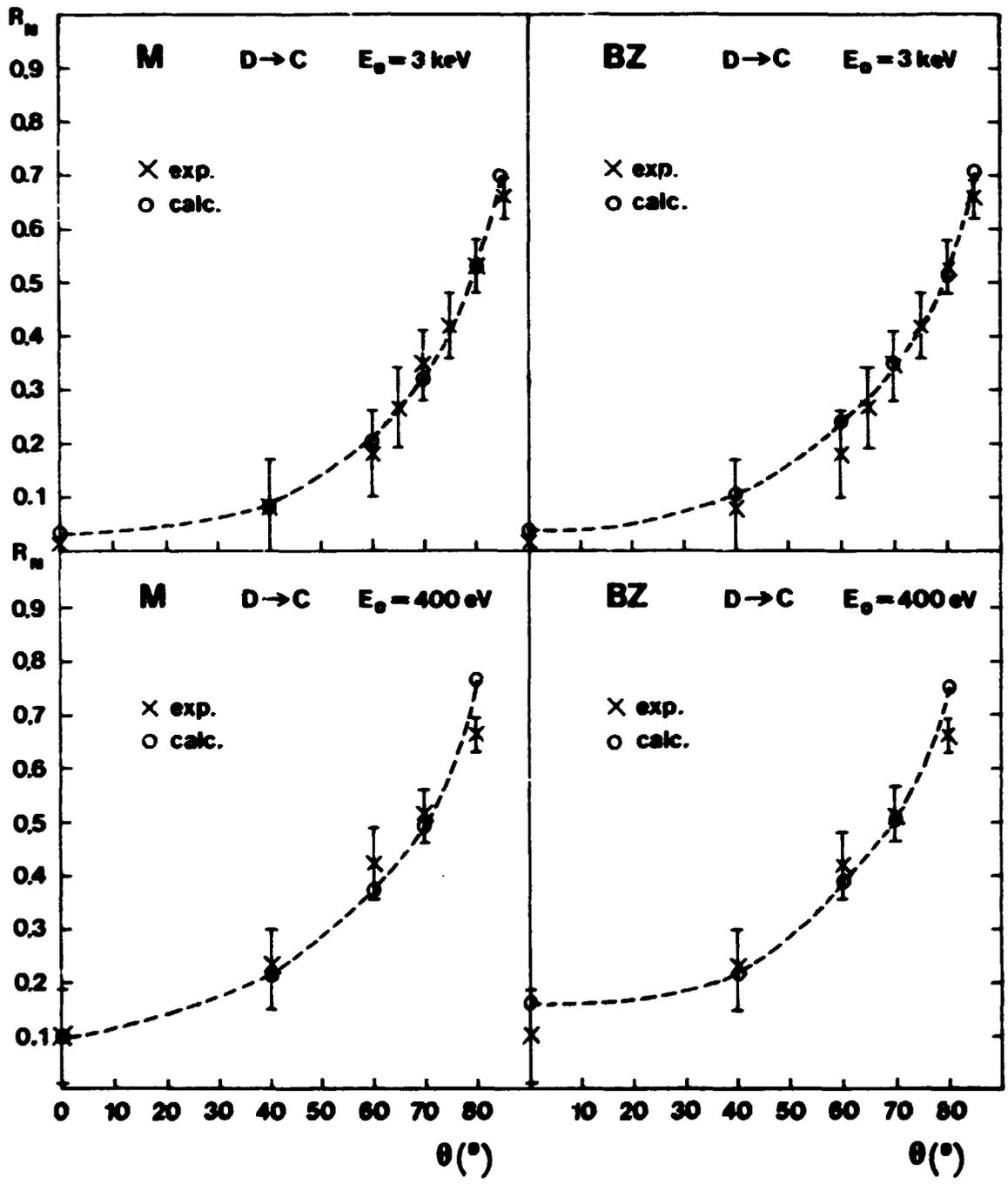

Fig.5: Particle reflection coefficient, R_N, for deuterium impinging on graphite, as a function of the angle of incidence θ; M: Molière; BZ: Biersack-Ziegler; the experimental data are from ref. [14].

Edito dall'ENEA. Direzione Centrale Relazioni
Viale Regina Margherita 125, Roma
Arti Grafiche F. Santarelli - Via Basento 81/83 - Roma